BALKAN JOURNAL OF ELECTRICAL & COMPUTER ENGINEERING, Vol. 14, 2026
Research Article

Investigation of Angle Measurement Errors in a PCB-Based Resolver Under Eccentricity Conditions

Fatih Sirli[1], Resat Celikel[2]

***Abstract*—Resolvers are widely employed in motor control applications such as industrial machinery, electric vehicles, and robotic systems to determine the motor shaft angle. In conventional resolvers with radial-flux and rotor-wound structures, rotor windings are typically used. However, in this study, these windings were replaced with a Variable Reluctance Rotor configuration to enhance performance. A new high-performance resolver based on an axial-flux design was proposed. The resolver windings were implemented on a printed circuit board (PCB), forming a compact and cost-effective structure. Finite Element Method (FEM) simulations were conducted to evaluate the design. To assess the resolver's performance, four different eccentricity conditions were introduced, and the system's performance under these conditions was analyzed. The simulation results are presented graphically, illustrating both the maximum and average measurement errors. Furthermore, the Total Harmonic Distortion (THD) of the sine and cosine output signals was evaluated to examine the influence of eccentricity-induced errors on signal quality.**

Index Terms— **PCB windings, Position measurement, Resolver, Variable Reluctance..**

I. INTRODUCTION

Electric motors are widely used in feedback-based industrial control systems. To determine the motor shaft position, various sensors such as encoders, hall-effect sensors, resolvers, and tachogenerators are used. Among these, resolvers are particularly preferred in applications requiring precise shaft-angle control due to their high stability, robustness, and superior noise immunity [1-2]. A resolver operates similarly to a rotating transformer, comprising one excitation (input) winding and two output windings arranged orthogonally. When a high-frequency sinusoidal voltage, typically in the range of 5–10 kHz, is applied to the excitation winding, two output voltages are induced that vary with the rotor's angular position. As illustrated in Figure 1, these output voltages correspond to the sine and cosine components of the rotor angle and are subsequently demodulated to generate pure sine and cosine signals. The instantaneous shaft angle of the motor can then be accurately determined from these demodulated signals [3-5].

Resolvers are manufactured in two different configurations, conventional rotor-wound and Variable Reluctance Resolvers (VRR), depending on their rotor structure. The most significant disadvantages of wound rotor resolvers are the risk of rotor-winding failures, the difficulty of rotor manufacturing, and poor performance in the event of axial misalignment. Because VRRs lack rotor windings, they have a lower risk of failure and are easier to manufacture, resulting in lower production costs [6-7]. Moreover, due to their shorter axial dimensions compared to wound-rotor resolvers, VRRs can be designed with more compact and lightweight structures. Different rotor, stator and winding structures have been developed to improve the angle measurement performance of VRRs. Various rotor and winding structures have been investigated in order to approximate the signals obtained from the output windings of VRRs to a sinusoidal waveform. In one design, various combinations were tested by varying the number of rotor poles and the number of stator teeth, and a new combination was proposed to reduce the angle error [8]. Another design method was developed to minimize the angle measurement error by using an asymmetrical stator and winding structure. This approach significantly reduced the angle error and demonstrated successful performance with a measurement error of 0.66˚ (0,0115 rad) [9]. A new VRR design was realized by using non-overlapping windings, a new winding structure that facilitates resolver manufacturing [10]. In a recent study, a hybrid excited linear VRR design that can operate in a wide speed range was operated [11].

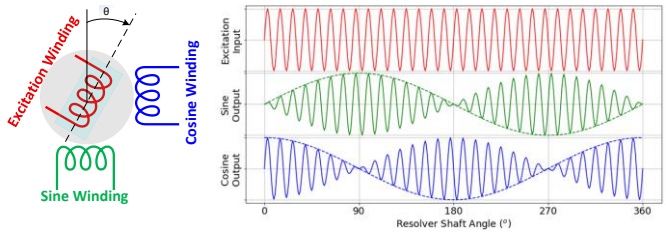


Fig.1. Input and output signals along with the structure of the resolver

When the literature is examined, it is seen that there are many studies on VRRs and that resolvers are divided into two groups according to the flux orientation type: radial flux and axial flux types [12]. Axial-flux resolvers stand out due to their ability to be manufactured with thinner structures and their lower angular measurement errors in the presence of axial misalignment. The Finite Element Method (FEM) analysis method is an important analysis method used in the design of electrical machines and is

[1] **Fatih Sirli**, is with Graduate School of Natural and Applied Sciences, Dept. of Mechatronics, Firat University, Elazig, Turkiye, (e-mail: fatihsirli23@hotmail.com). https://orcid.org/ 0009-0006-3976-9214
[2] **Resat Celikel**, is with Department of Mechatronic Engineering, Technology Faculty, Firat University, Elazig, Turkiye (e-mail: rcelikel@firat.com). https://orcid.org/ 0000-0002-9169-6466
Manuscript received Dec16, 2025; accepted March 26, 2026. DOI: 10.17694/bajece.1843179

Sihirli F. and Celikel R. (2026). Investigation of Angle Measurement Errors in a PCB-Based Resolver Under Eccentricity Conditions. Balkan Journal of Electrical and Computer Engineering, 14, 11-19.

Copyright © BAJECE

also widely used in resolver design [13]. Axial misalignment in the rotor remains is a major challenge.

Axial misalignment in the rotor represents a significant issue. To mitigate the errors arising from static and dynamic misalignments, a resolver including a damper winding has been developed. The performance of the proposed resolver was validated through both experimental and FEM-based simulation studies, demonstrating its effectiveness. Under perfect alignment conditions, the maximum measurement error was reported as 0.208° (0.0036 rad) [14]. An axial-flux resolver with a disc-type rotor was designed in three different noise-resistant configurations: 2, 4, and 6 poles. The maximum measurement error of the designed resolver was approximately 0.34° (0.0059 rad), while the average error was 0.07° (0.0012 rad) [15]. In another important study, the winding function of the axial-flux resolver was optimized using a genetic algorithm, resulting in a maximum measurement error of 0.33° (0.0057 rad), while the average error was 0.08° (0.0014rad) [16]. Experimental results have further demonstrated that axial-flux resolvers exhibit lower angular measurement errors under axial misalignment compared to radial-flux resolvers, even with simpler designs [17]. Additionally, a magnetic model was developed for an axial-flux VRR with a distinct rotor structure and compared with a time-stepped finite element (FE) model, showing close agreement between the two approaches. Experimental validation yielded a maximum measurement error of 0.2° (0.0035 rad) [18].

In recent years, PCB (Printed Circuit Board) based resolvers have gained importance due to their thin structure and low failure risk. In these resolvers, the rotor is made with variable reluctance structure, while the excitation and induction windings are placed on the printed circuit board. PCB-based resolvers are not only easy to manufacture but also cost-effective. Owing to their axial-flux design, they can be produced in extremely thin configurations. In the literature, such sensors are often referred to as inductive position sensors; however, their operating principle is essentially the same as that of conventional resolvers. A low-cost resolver structure, where the rotor and stator windings are each implemented on a single PCB, was developed, achieving an angle measurement error of 5.625˚ (0.098 rad) [19]. In similar studies, a PCB-based resolver with a different rotor configuration was designed, achieving an experimental angular measurement error of 0.125˚ (0.00218 rad) [20]. In another study, a new inductive position sensor, also known as a resolver, with an optimized winding structure was introduced. After optimization, the maximum angle measurement error of this sensor was reported to be 0.1˚ (0.0017 rad) [21].

In a recent study, a hybrid resolver was introduced in which the windings were formed on a PCB, while the rotating rotor consisted of a 4-pole permanent magnet. The maximum measurement error of the hybrid resolver was reported as 0.25° (0.0043 rad) [22]. An axial flux hybrid resolver with a permanent magnet stator was developed. Comparisons were made between different rotor designs by forming the resolver windings on a PCB. Experimental results showed that the maximum measurement error was below 5° at high speeds such as 10,000 rpm [23]. In a very recent study, a lightweight and thin PCB-VRR was introduced. Square-wave excitation simplified the excitation process, and angle measurements were also performed with a microcontroller to controlling the motor. The resolver operated at high speeds with a measurement error of 0.6° (0.0104 rad) [24]. A new PCB-based resolver, in which the rotor and stator windings were formed on a PCB, was also introduced to facilitate rotor fabrication. In this study, the measurement error was quite low, and the resolver was tested at both low and high speeds [25]. A review of the literature reveals that eccentricity errors in PCB-based resolvers have not been studied. This study analyzes eccentricity errors along with a very thin resolver design. The effect of eccentricities occurring in the x, y, and z axes, especially during assembly, on resolver errors in thin resolvers is demonstrated.

Firstly, an axial-flux PCB-based resolver was modeled and simulated using FEM under ideal conditions, without any misalignment. In the second stage, misalignments were introduced in the x and z directions, and the simulations were repeated. The obtained results were analyzed in the MATLAB environment and compared with the reference angle. By examining the measurement errors and the Total Harmonic Distortion (THD) values of the output signals obtained from the simulations, the effects of various mechanical imperfections on the measurement system were evaluated.

II. PCB-BASED RESOLVERS

Conventional resolvers consist of three windings, a stator, and a rotor. The resolver operates based on the principle of electromagnetic induction and functions similarly to a rotating transformer. As in a transformer, the resolver includes primary and secondary windings. There are two secondary windings, which are placed at a geometric angle of 90˚ to each other. When a high-frequency sinusoidal input is applied to the primary winding, two output voltages proportional to the sine and cosine of the rotor position are obtained from the secondary windings. Since the resolver's rotor is mechanically coupled to the motor shaft, the voltages induced in the output windings contain information about the motor shaft angle. After converting the output signals to sine and cosine signals using a modulation process, the motor shaft angle is obtained using a simple trigonometric expression. The voltages induced in the secondary windings, which are proportional to the input signal and the rotor displacement, are given in Equations (1) through (3).

$$V_p(t) = V_m \sin(\omega_e t) \tag{1}$$

$$V_s(t) = K_i V_m \sin(\omega_e t) \sin(\theta) \tag{2}$$

$$V_c(t) = K_i V_m \sin(\omega_e t) \cos(\theta) \tag{3}$$

where ω_e denotes the angular frequency of the input voltage and has a high frequency. K_i represents the resolver constant, V_m is the maximum value of the primary-side voltage, and θ denotes the rotor angle. As shown in Figure 1, the maximum value of the sinusoidal voltage obtained from the secondary side, which varies in each period, is sampled to derive the sine and cosine signals. The sampled sine and cosine signals seen in Figure 1 appear as signals that change depending on the motor angle. As seen in Equation 4, the position of the motor shaft angle is obtained from these signals with the arctan trigonometric process. Various algorithms and methods are used to obtain the angle value with the least error. The amplitude of the output signals varies depends on the number of turns of the excitation and induced windings, as well as on the rotor structure.

$$\theta = arctan\left(\frac{K_i V_m \widehat{sin(\theta)}}{K_i V_m \widehat{cos(\theta)}}\right) \tag{4}$$

A variable-reluctance rotor structure is used in the PCB-based resolver. The amplitude of the output signals depends on the number of turns of the excitation and induced windings, as well as on the rotor structure. In the PCB-based resolver, both the excitation and output windings are placed on the same printed circuit board. By manufacturing the rotor from a very thin metal sheet, a much thinner resolver design is achieved compared to conventional resolvers. The most significant limitation of PCB-based resolvers is that the number of winding turns cannot be substantially increased. Increasing the number of turns would require adding more layers to the PCB, which in turn would increase manufacturing costs.

In the designed PCB-based resolver, the excitation winding is a single-piece, spiral-shaped coil located on the outer surface, while the secondary windings are designed as two separates parts. The winding directions of the two parts windings are determined to be opposite to each other. The EMFs induced in the split winding are therefore opposite to each other, as shown in Equation (5), where N_1 represents the number of turns in one half of the split winding, while N_2 represents the number of turns in the other half. I_1 and I_2 represent the currents in the first and second windings, respectively.

$$\mathcal{F}_{SC} = N_1 I_1 - N_2 I_2 \tag{5}$$

In this type of resolver structure, the induced voltages depend not only on the field-winding flux and current, but also on the mutual inductance between the two windings. Equation (6) shows the field-winding current, and Equations (7) and (8) represent the induced voltages.

$$I_e = I_{max} * \sin(\omega t) \tag{6}$$

$$V_{sc} = M \frac{dI_e}{dt} \tag{7}$$

$$V_{SC} = M * \omega * I_{max} * \cos(\omega t). \tag{8}$$

where, $I_{\max}$ represents the maximum value of the excitation current, ω denotes the frequency of the excitation current, and M indicates the mutual inductance between the excitation winding and the induction coils used for angle measurement. The mutual inductance also varies according to the rotor position. Depending on the variation of the mutual inductance, output voltages that change with the rotor position are obtained from the output windings.

The PCB winding is mounted on a stator made of 1010 steel which is designed according to the shape of the circuit board, in order to increase the level of the induced voltage.

III. SIMULATION OF THE PCB-BASED RESOLVER

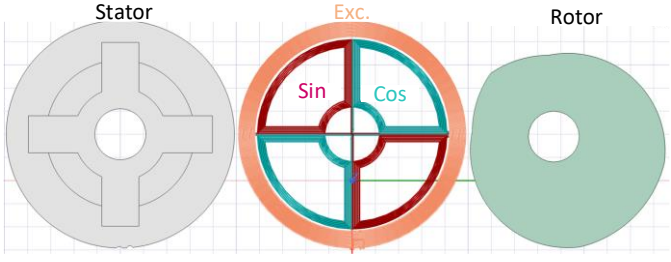


Fig.2. Stator, windings and rotor of simulated PCB-based solver

The amplitude of the induced voltages is determined by the rotor position, field current, mutual inductance, and the angular velocity of the voltage applied to the field coil. The frequency of the field-winding voltage was set at 10 kHz, and the peak value was set at 5 V. A two-layer winding structure was chosen to increase the induced voltage. Because the rotor is mechanically connected to the motor shaft, the rotor speed was set at 10,000 rpm, and the simulation sampling interval was set at 10 μs. The PCB windings, stator, and rotor structure designed in the ANSYS program are shown in Figure 2.

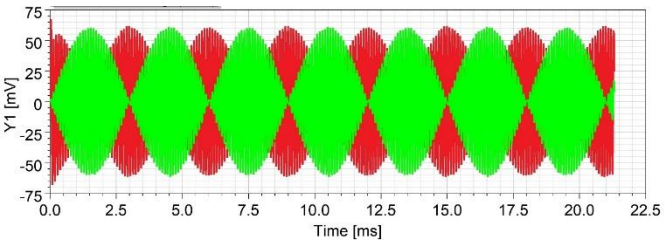


Fig.3. Resolver output signals obtained from error-free resolver FEM simulation.

The outer diameter of the PCB winding was determined to be 53.5 mm. The excitation winding was designed with 10 turns per layer, comprising a total of 40 turns. The sine and cosine output windings were each designed with 5 turns per layer and a total of 20 turns. The stator was positioned 1 mm inward, centred between the gaps of the sine and cosine windings. The rotor was designed to be manufactured from 0.5 mm thin sheet metal, and the total thickness of the PCB-based resolver was 2.5 mm. The fundamental advantage of PCB resolvers, their thinness, is demonstrated in this study.

Figure 3 presents the output signals obtained from the simulation study, which exhibit a peak amplitude of approximately 60 mV. As shown in Figure 4, after transferring the output signals to the MATLAB environment, the peak points were sampled to obtain the sine and cosine signals. Figure 5 illustrates a comparison between the calculated motor shaft angle, derived from the sine and cosine signals, and the actual motor shaft angle. The maximum measurement error of the designed resolver was determined to be 0.0228 rad (1.3°). When analyzing axis misalignment errors, knowledge of the actual measurement error of the resolver contributes to a more accurate interpretation of the results. Additionally, the harmonic content of the sine and cosine signals was calculated as shown in Figure 6.

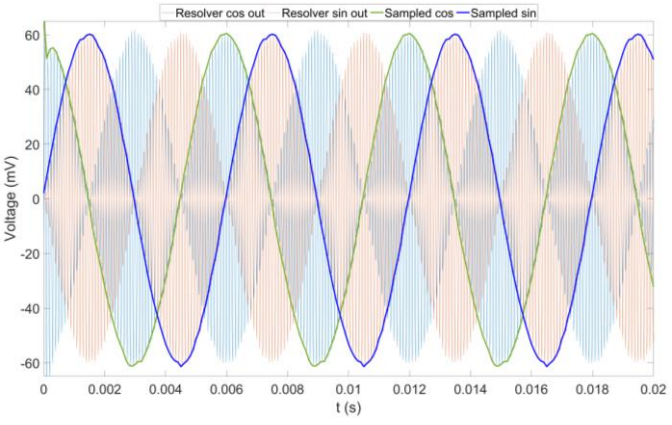


Fig.4. Resolver output signals with sampled peak pointsobtained from error-free resolver FEM simulation.

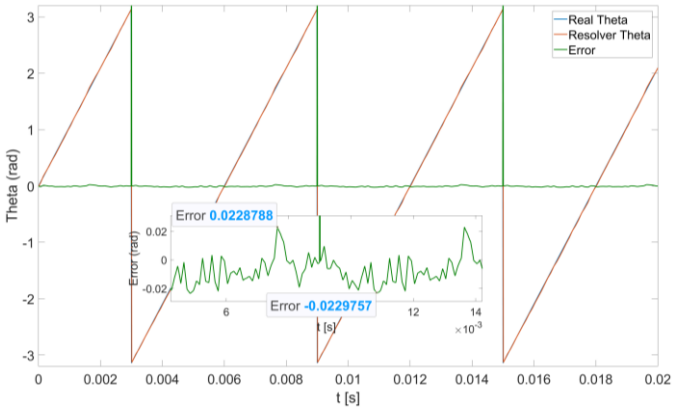


Fig.5. Shaft angle measured by the resolver under normal conditions and its measurement error.

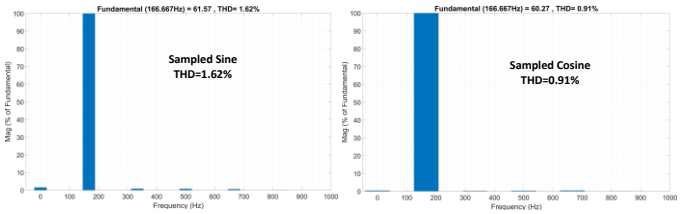


Fig.6. Harmonic content of the resolver output signals. obtained from error-free resolver FEM simulation.

IV. ECCENTRICITY AND SIMULATION RESULTS

As shown in Figure 7, resolvers have two types of eccentricity errors: static eccentricity, which occurs when the rotor rotates without misalignment but is caused by manufacturing defects or stator placement errors, and dynamic eccentricity, which occurs when the rotor shifts from the motor shaft axis during assembly. This study focuses on dynamic eccentricity errors. Another potential source of error during the installation of the resolver rotor is the non-uniform air gap between the PCB surface and the rotor surface.

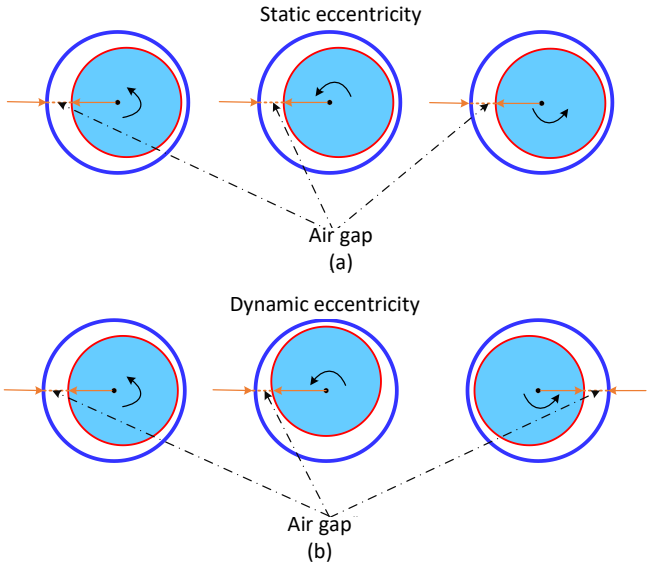


Fig.7. Possible eccentricity errors in the resolver rotor.

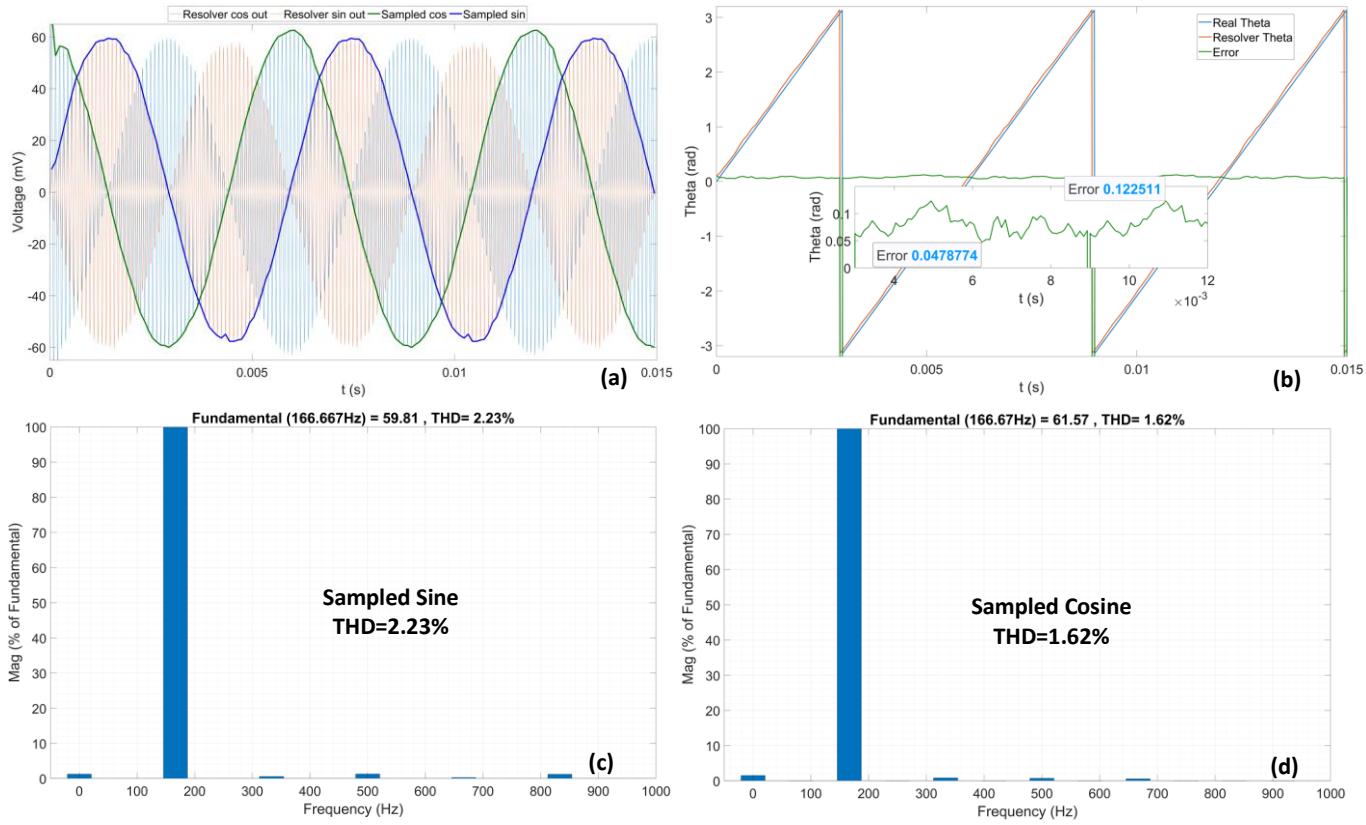


Fig.8. Resolver rotor with 0.5 mm eccentricity along the x-axis: (a) Resolver output signals, (b) Angular measurement error, (c) THD of sine output signal, (d) THD of cosine output signal.

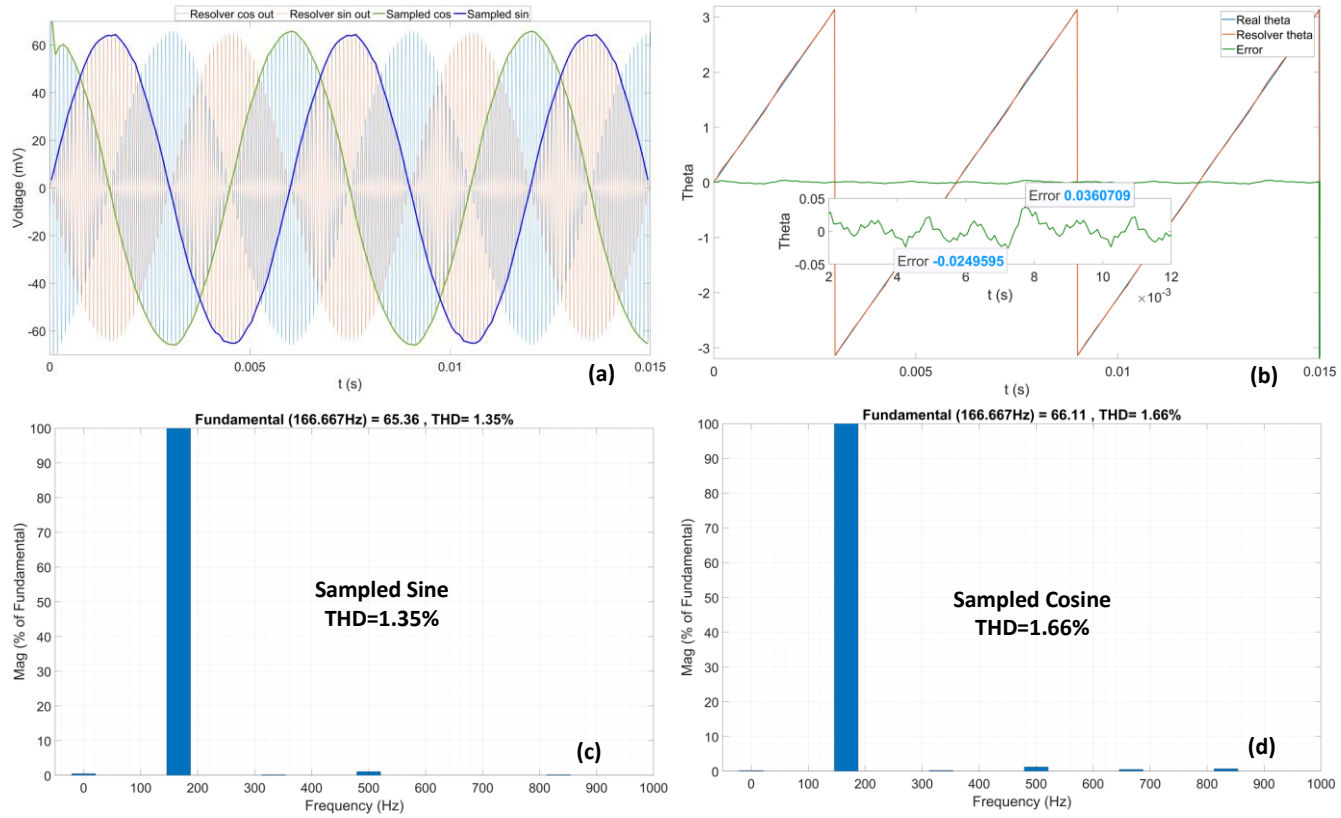


Fig. 9. Resolver rotor with 0.5 mm eccentricity along the x and y axis: (a) Resolver output signals, (b) Angular measurement error, (c) THD of sine output signal, (d) THD of cosine output signal.

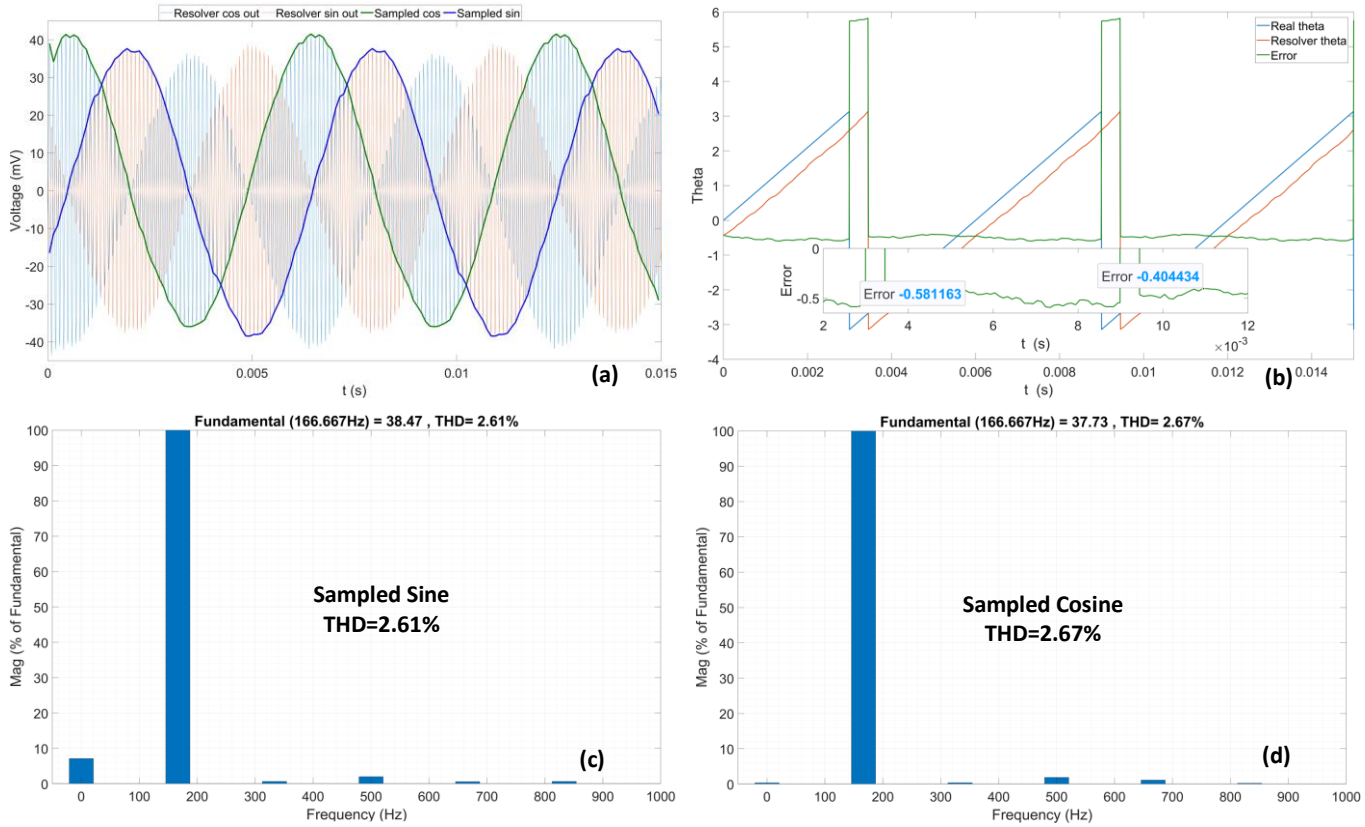


Fig.10. Resolver rotor with 0.5 mm positioning error on the z-axis: (a) Resolver output signals, (b) Angular measurement error, (c) THD of sine output signal, (d) THD of cosine output signal.

In this study, the rotor axis misalignment in the x and y directions, as well as the positioning error in the z direction, were investigated by creating four different cases. Figure 8 presents the simulation results for the case in which the rotor is assumed to be displaced by 0.5 mm along the x-axis. In industrial applications, an axial misalignment of 0.5mm without assembly errors is a significant value. In this study, considering eccentric misalignments caused by assembly errors, a large axial misalignment value has been selected. As shown in Figure 8(a), the distortion in the sine output signal is clearly noticeable. In

Figure 8(b), the maximum measurement error increases to 0.0478 rad, while Figures 8(c) and 8(d) illustrate that the increase in the THD values of the sine and cosine output signals indicates greater distortion in the output waveforms. The average angular measurement error was calculated to be 0.0166 rad.

Figure 9 presents the simulation results assuming a 0.5 mm simultaneous displacement of the rotor along both the x and y axes. In Figure 9(a), the distortion in the sine and cosine signals is not clearly observable. However, the distortion in the output signals is visible with the decrease in THD in Figure 9(c) and the increase in THD in Figure 9(d). As seen in Figure 9(b), the maximum measurement error has increased to 0.036 rad. The average measurement error was calculated to be 0.0024 rad, and it was observed that the misalignment in the x and y directions did not cause a significant change in the average error.

Figure 10 shows the results of the simulation performed for a 0.5 mm placement error along the rotor's z-axis. The distortion in the sine and cosine signals is clearly visible in Figure 10(a). The increase in the THD value in the signals is shown in Figures 10(c) and 10(d). The maximum measurement error was -0.581 rad, as shown in Figure 10(b). The average measurement error was calculated to be -0.5013 rad.

Figure 11 shows the results of a simulation performed with a 0.5 mm rotor placement error along the x-axis and a 0.5 mm rotor placement error in the z-axis. Figure 11(a) clearly demonstrates the distortion in the sine and cosine signals. The THD values in the sine and cosine output signals increased by 1.91% and 3.38%, respectively, as shown in Figures 11(c) and 11(d),. The maximum measurement error was -0.581 rad, as shown in Figure 11(b). The average measurement error was calculated to be -0.5303 rad.

The simulation results, conducted by examining four different error conditions, are summarized in Table I. Accordingly, it can be seen that a rotor mounting error in the z-direction has a significant impact on the measurement system. It was observed that axial misalignments in the x and y directions increase the measurement error, but a lower measurement error occurs compared to the mounting error in the z-direction. The simulation study shows that the largest measurement error occurs in z-axis misalignment. PCB-based resolvers, in particular, are difficult to assemble due to their thin structure. Various methods are continuously being developed to ensure error-free assembly. Since z-axis errors cause very large errors, they need to be minimized in real industrial applications. For this purpose, magnetic field sensing systems have been created in some types of resolvers to reduce z-axis misalignment and detect z-axis errors. From this perspective, developing new designs to reduce z-axis misalignment in PCB resolvers should be the subject of future research.

Table I. Simulation results for four error conditions

Eccentricity	Sin THD%	Cos THD%	Max. Err. (rad)	Mean Err. (rad)
X (0.5mm)	2.23	1.62	0.122	0.0166
X and Y (0.5mm)	1.35	1.66	0.036	0.0024
Z (0.5mm)	2.61	2.67	-0.581	-0.501
X and Z (0.5mm)	1.91	3.38	-0.581	-0.530

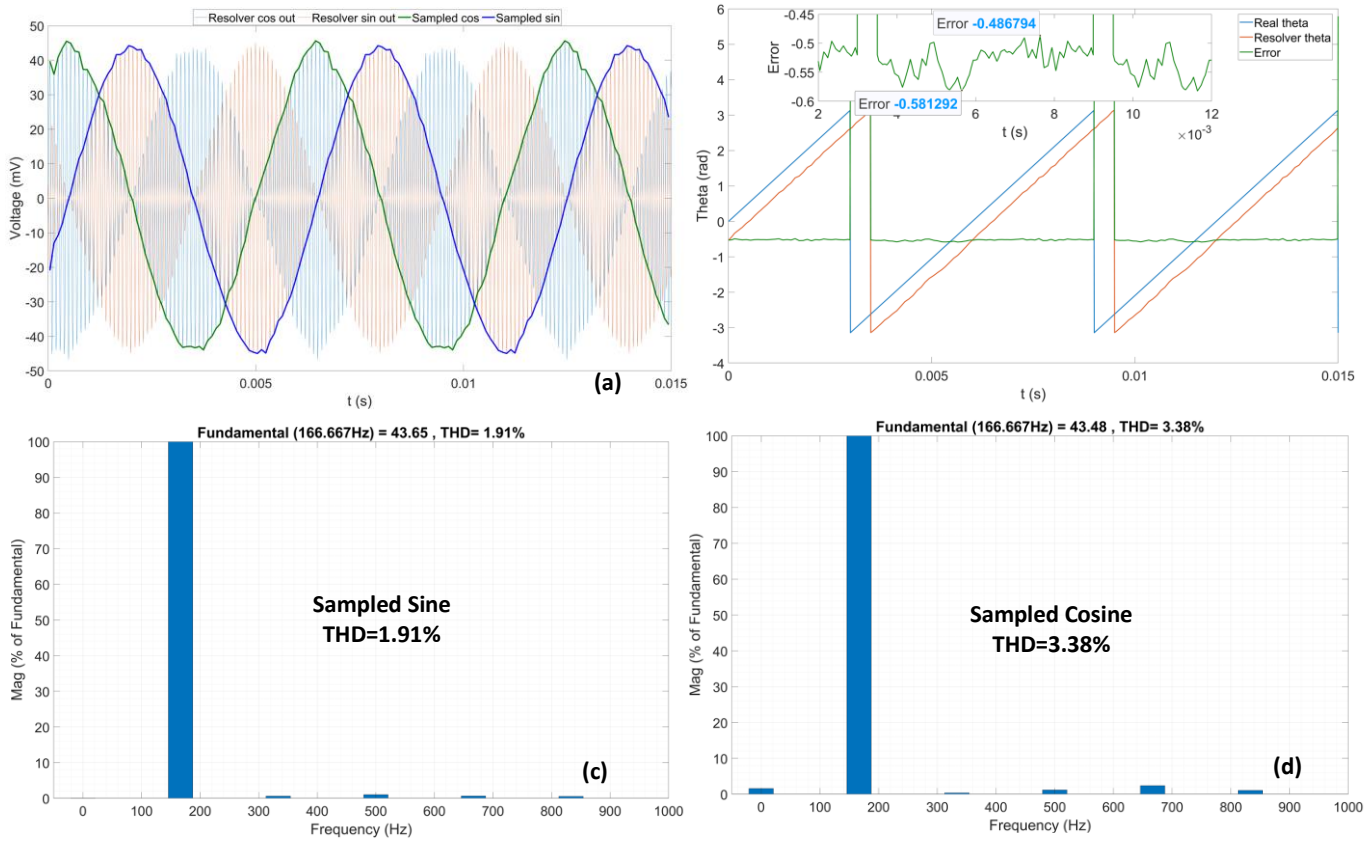


Fig. 11. Resolver rotor with 0.5 mm eccentricity on the x-axis and a 0.5 mm positioning error on the z-axis. (a) Resolver output signals, (b) Angular measurement error, (c) THD of sine output signal, (d) THD of cosine output signal.

V. CONCLUSION

Resolvers are widely used in industrial control systems to determine motor shaft angle. By eliminating the rotor windings in conventional resolvers and adopting VRR designs, resolvers that are more robust to noise and failures have been developed. The absence of rotor windings also enables thinner constructions. It has been demonstrated in the literature that axial-flux resolvers are more advantageous than conventional resolvers with respect to rotor positioning errors and eccentricity faults. In PCB-based resolvers, all windings are placed on a single PCB, and the rotor is designed with variable reluctance, resulting very thin and highly fault-tolerant resolvers have been developed.

In this study, the behaviour of an axial-flux PCB-based VRR design under axis-misalignment errors is analysed. A FEM model was used in the simulation study. While the PCB windings were designed as four layers, the rotor was constructed from 0.5 mm thin sheet metal, resulting the total resolver thickness was created as very thin as 2.5 mm. Analysis under four different error conditions indicated that distortion in the output signals was most significant for the z-axis mounting error, with a maximum measurement error of -0.581 rad. In cases where eccentricity occurred simultaneously along the x and y axes, the maximum measurement error was observed to be 0.036 rad, which is lower compared to the other three cases.

This study shows that a very thin resolver can be designed by constructing the rotor from thin sheet metal, while also highlighting that large maximum errors occur along the z-axis eccentricity in PCB-based resolver. Simulation studies have shown that the maximum measurement error is lower when eccentricity errors in the x and y axes occur simultaneously. In future studies, additional measures will be implemented to reduce errors in the z-axis during resolver assembly, including the development of specialized assembly equipment and a z-axis misalignment error detector.

ACKNOWLEDGMENT

This study was produced from the first author's Master's thesis titled 'Analysis of Eccentric Errors in a Printed Circuit Board-Based Resolver'.

REFERENCES

[1] Benammar, M., Ben-Brahim, L., & Alhamadi, M. A. (2005). A high precision resolver-to-DC converter. IEEE Transactions on Instrumentation and Measurement, 54(6), 2289-2296.

[2] Benammar, M., Ben-Brahim, L., & Alhamadi, M. A. (2004). A novel resolver-to-360° linearized converter. IEEE Sensors Journal, 4(1), 96-101.

[3] Ben-Brahim, L., Benammar, M., & Alhamadi, M. A. (2008). A resolver angle estimator based on its excitation signal. IEEE transactions on industrial electronics, 56(2), 574-580.https:// doi.org/10.1109/TIE.2008.2002719.

[4] Celikel, R. (2019). ANN based angle tracking technique for shaft resolver. *Measurement*, *148*, 106910

[5] Celikel, R., Boztas, G., & Aydogmus, O. (2023). An investigation on the position errors of resolvers designed in different structures: A review. Measurement, 218, 113186.

[6] Tootoonchian, F., & Zare, F. (2023). Sinusoidal area 2-DoF variable reluctance resolver. IEEE Sensors Journal, 24(2), 1358-1365.

[7] Kim, K. C. (2013). Analysis on the charateristics of variable reluctance resolver considering uneven magnetic fields. IEEE Transactions on magnetics, 49(7), 3858-3861.

[8] Ge, X., Zhu, Z. Q., Ren, R., & Chen, J. T. (2015). Analysis of windings in variable reluctance resolver. IEEE transactions on magnetics, 51(5), 1-10.

[9] Liu, C., Qi, M., & Zhao, M. (2013). Analysis of Novel Variable Reluctance Resolver with Asymmetric Teeth on the Stator. Mathematical Problems in Engineering, 2013(1), 958747.

[10] Ge, X., Zhu, Z. Q., Ren, R., & Chen, J. T. (2014). A novel variable reluctance resolver with nonoverlapping tooth–coil windings. IEEE Transactions on Energy Conversion, 30(2), 784-794.

[11] Moghaddam, G. S., Nasiri-Gheidari, Z., & Alipour-Sarabi, R. (2024). Hybrid excitation for a wide speed range linear sinusoidal area variable reluctance resolver. IEEE Transactions on Instrumentation and Measurement, 73, 1-7.

[12] Nasiri-Gheidari, Z., & Tootoonchian, F. (2015). Axial flux resolver design techniques for minimizing position error due to static eccentricities. IEEE Sensors Journal, 15(7), 4027-4034.

[13] Tootoonchian, F. (2018). Proposal of new windings for 5-X variable reluctance resolvers. IET Science, Measurement & Technology, 12(5), 651-656.

[14] Tootoonchian, F. (2018). Proposal of a new affordable 2-pole resolver and comparing its performance with conventional wound-rotor and VR resolvers. IEEE Sensors Journal, 18(13), 5284-5290.

[15] Nasiri-Gheidari, Z., Alipour-Sarabi, R., Tootoonchian, F., & Zare, F. (2017). Performance evaluation of disk type variable reluctance resolvers. IEEE Sensors Journal, 17(13), 4037-4045.

[16] MAlemi-Rostami, M., Alipour-Sarabi, R., Rezazadeh, G., Nasiri-Gheidari, Z., & Oraee, H. (2019). Design optimization of a double-stage resolver. IEEE Transactions on Vehicular Technology, 68(6), 5407-5415.

[17] Chang, T. W., Huang, P. W., Huang, W. C., Huang, C. C., Mo, C. C., & Tsai, M. C. (2023). Additive manufacturing high fault-tolerant axial flux variable reluctance resolver. IEEE Transactions on Magnetics, 59(11), 1-5.

[18] Saneie, H., Nasiri-Gheidari, Z., & Tootoonchian, F. (2017). Design-oriented modelling of axial-flux variable-reluctance resolver based on magnetic equivalent circuits and Schwarz–Christoffel mapping. IEEE Transactions on Industrial Electronics, 65(5), 4322-4330.

[19] Gao, W., Shi, H., & Tang, Q. (2021). A contactless planar inductive sensor for absolute angular displacement measurement. IEEE access, 9, 160878-160886.

[20] Tang, Q., Peng, D., Wu, L., & Chen, X. (2015). An inductive angular displacement sensor based on planar coil and contrate rotor. IEEE Sensors Journal, 15(7), 3947-3954.

[21] Hoxha, A., Passarotto, M., Qama, G., & Specogna, R. (2022). Design optimization of PCB-based rotary-inductive position sensors. Sensors, 22(13), 4683.

[22] Brajon, B., Lugani, L., & Close, G. (2022). Hybrid magnetic–inductive angular sensor with 360° range and stray-field immunity. Sensors, 22(6), 2153.

[23] Sun, L., Luo, Z., Hang, J., Ding, S., & Wang, W. (2021). A slotless PM variable reluctance resolver with axial magnetic field. IEEE Transactions on Industrial Electronics, 69(6), 6329-6340.

[24] Sun, L., Kong, T., Wu, C., Zhang, L., Wang, W., & Ding, S. (2023). The leaf-style axial field variable reluctance resolver with an efficient decoding system. IEEE Transactions on Industrial Electronics, 71(9), 11581-11591.

[25] Hajmohammadi, S., & Nasiri-Gheidari, Z. (2024). Proposal of a wound-rotor PCB-resolver. IEEE Transactions on Industrial Electronics, 71(11), 15122-15129.

[26] Deng, W., Zhao, C., Xiao, G., Qian, Z., Li, G., Chen, Q., & Wang, Q. (2025). Influence of eccentricity on the position error of variable reluctance resolvers based on the winding function method. IEEE Sensors Journal, 25(5), 8417-8432.

[27] Park, S., Kim, J., Kwon, W., Kang, J., & Kim, N. (2025). Mechanical fault detection and classification in variable reluctance resolver based on Lissajous curve indices. Measurement, 118631.

[28] Naderi, P. (2023). A novel variable-reluctance resolver proposal and its performance analysis under healthy and eccentric cases. Mechatronics, 90, 102948.

BIOGRAPHIES



Fatih Sirli was born in 1976. He received the B.S. degrees in Electrical Education from the University of Firat, Elazig, Turkey. He is studying for his master's degree in mechatronic engineering at Firat University. His research interests include electric machinery and Resolver.



Resat Celikel was born in 1980. He received the B.S., M.S., and Ph.D. degrees from Firat University, Elazig, Turkey. He has been an Associate Professor with Firat University. His current research interests include BLDC motors, flywheel energy storage, FPGA, renewable energy, and MPPT